PHARMA RESEARCH BULLETIN
Open Access Journal (ISSN: 2582-676X)

Research article
Volume 3, 2021, 08-17

Design and Synthesis of A Newer Series of Caffeic Acid Analogs as Potential New Delhi Metallo-β-Lactamase-1 (NDM-1) Inhibitors

Meenu Verma [1], Ajmer Singh Grewal [2*], Deepti Pandita [3], Viney Lather [4]

[1] Jan Nayak Ch. Devi Lal Memorial College of Pharmacy, Sirsa, Haryana, India
[2] Guru Gobind Singh College of Pharmacy, Yamunanagar, Haryana, India
[3] Department of Pharmaceutics, Delhi Pharmaceutical Sciences and Research University, Pushp Vihar, New Delhi, India
[4] Amity Institute of Pharmacy, Amity University, Noida, Uttar Pradesh, India

* Correspondence: ajmergrewal2007@gmail.com; ajmer.singh@gnkgei.ac.in

Received: 15 March 2021; Accepted: 18 June 2021; Published: 25 June 2021

Abstract: New Delhi metallo-β-lactamase-1 (NDM-1) constructing microorganisms are unaffected by all the β-lactams together with carbapenems and pose an extreme risk to community wellbeing as they can simply spread through horizontal gene transfer. The present work was planned to design, prepare and evaluate the novel caffeic acid analogues as potential NDM-1 inhibitors. Docking studies were accomplished for exploring the binding interactions of the designed molecules in the active site of NDM-1 protein. A newer series of azetidine-substituted caffeic acid derivatives were synthesized using microwave irradiation and characterized using FTIR and ^{1}H NMR spectroscopy. Designed molecules showed appreciable hydrogen bonds with Asn220 and metal interactions with zinc ions in the active site of NDM-1. Compounds 1, 6, 9 and 14 showed powerful *in vitro* antibacterial activities against *Escherichia coli* and compounds 4 and 13 showed potent antibacterial activities against *Pseudomonas aeruginosa*. The preliminary *in silico* results shows an enormous potential for these molecules to act as strong NDM-1 inhibitors.

Keywords: Antibiotic resistance; Antibacterial activity; Caffeic acid derivatives; New Delhi metallo-β-lactamase-1; NDM-1 inhibitors.

1. Introduction

The appearance of antibiotic resistance in bacteria has resulted in a histrionic fading of the value of antibiotics. The predominant pathways of antimicrobial resistance consist of decreased permeability of cell walls, antibiotic efflux and enzyme-facilitated drug deprivation (Tang et al., 2014; Hawkey, 2015; Kumar et al., 2018). Escorted by the global usage of β-lactam antimicrobials, β-lactamase-facilitated resistance to antibiotics has pinched continually increased worry as the genes encoding β-lactamase are generally placed on transportable parts and simply unfurl amongst the microbes (Papst et al., 2018). Grounded on their molecular characteristics and/or amino acid residues, the β-lactamase enzymes are classified into A, B, C and D types, with types A, C and D demonstrating hydrolysing ability dependent on the serine residue. Type B needs either 1 or 2 Zn ions as the nucleophile and accordingly is recognized as metallo-β-lactamase (MBL) enzymes (Ambler et al., 1985). The MBL enzymes are of 3 subtypes (B1, B2 and B3), and out of these subtypes, B1 New Delhi metallo-β-lactamase-1 (NDM-1) had engrossed widespread courtesy in the past decade as it deliberates resistance against practically all types of β-lactams except the monobactam aztreonam (Johnson et al., 2013). NDM-1 is programmed on eagerly moveable plasmid DNA, simplifying its spread (Kumarasamy et al., 2010; Sidjabat et al., 2011; Fair and Tor, 2014). Current investigation has recommended that the ^{bla}NDM-1 gene deliberating antimicrobial resistance is nowadays broadly transmission globally. Presently, 20 variants of the NDM-1 enzyme were documented, whereas no operative inhibitor of NDM-1 (or MBLs) is available clinically (Liu et al., 2017). Pathogens possessing ^{bla}NDM-1 may cause an actual and challenging menace to human well-being in the coming future (Rogers et al., 2013). Identifying novel inhibitors of NDM-1 as antibiotic adjuvants is vital to prevent upcoming disastrous diseases (Shlaes, 2013; Linciano et al., 2019). The

grouping of an inhibitor of serine-β-lactamase with a β-lactam antibiotic was employed for the management of antimicrobial drug-resistant contaminations clinically. Though the inhibitors of serine-β-lactamase (for instance potassium clavulanate or sulbactam sodium) posed no outcome on the MBL enzymes, whereas metal ion chelating agents (like disodium EDTA, 1,10-phenanthroline and dipicolinic acid) had no medical implication due to their adverse reactions (Aoki et al., 2010; King and Strynadka, 2013). Numerous chemical scaffolds including both natural as well as synthetic compounds demonstrated effective inhibitory potential against NDM-1 in the past decade (Grewal et al., 2020). Still, not a single MBL inhibitor was approved for clinical use (Rotondo and Wright, 2017). Due to the speedy transmission of the NDM-1 enzyme worldwide, identifying and developing novel inhibitors of NDM-1 with high effectiveness is predominantly crucial (Shi et al., 2019). Based on the role of NDM-1 in antibiotic resistance, we have attempted to design and prepare a series of novel caffeic acid derivatives as NDM-1 inhibitors.

2. Materials and Methods

All the chemicals were procured from Otto Chemie, Spectrochem, Sigma etc., and used without further purification. Discover microwave synthesizer (CEM Corporation) was utilized to carry out the "microwave-assisted reaction". Melting points were determined using the "Veego VMP-D" melting point determination device. The accomplishment of the reaction was checked through single-spot TLC. "Bruker Avance II 4000 MHz NMR Spectrophotometer" was employed to record the ^{1}H-NMR spectra and documented as the chemical shift (δ) in ppm down-field from the internal standard. FTIR spectrophotometer was used to determine the FTIR spectra by using the KBr pellet method.

2.1. Synthesis of the caffeic acid analogues

2.1.1. Preparation of substituted caffeoyl amide derivatives: A mixture of substituted benzaldehydes (7.8 mmol), pyridine (49.4 mmol), malonic acid (19.2 mmol) and piperidine (0.2 ml) was heated on a water bath for 3 h. The reaction mixture was then poured into 2N HCl. The acid precipitated instantly and was permitted to stand for a few minutes followed by filtration and drying. The substituted caffeic acids (0.1 mmol) obtained above were then refluxed with $SOCl_2$ (0.1 mmol) for 4 h followed by refluxing with NH_3 (0.l mmol) for 3 h and the product was air dried (Kavitha et al., 1999).

2.1.2. Preparation of 2,4-dibromo-N-hydroxybutanamide: Phosphorus tribromide (1 ml) was added to 4.37 mL of γ-butyrolactone followed by heating to 100 ˚C. The mixture was stirred and 2.6 ml of Br_2 was added dropwise (3 h) beneath the surface of the liquid maintaining temperature at 110-115 ˚C during the first 1 h. More PBr_3 (0.25 ml) was then added and the reaction temperature was maintained for 1.5-2 h with stirring followed by cooling to room temperature. Hydroxylamine (3.8 g) was added to the above product using toluene as solvent and the system was refluxed for 30 min. In the end, toluene was evaporated and 2,4-dibromo-N-hydroxybutanamide was collected (Wagner et al., 1955).

2.1.3. Preparation of 2,4-dibromo-N-hydroxy-4-phenylbutanamide: Phenyl butyric acid (0.01 mol) was refluxed for 25 min with N-bromosuccinimide (0.011 mol) and benzoyl peroxide (7.5 mmol) and CCl_4 was used as a solvent. After completion of the reaction, the insoluble imide floating over the reaction mixture was removed by filtration. CCl_4 (solvent) was evaporated and crystals were collected. These crystals (0.01 mol) were reacted with Br_2 (0.011 mol) in a flask and when the temperature touched 65 ˚C, PCl_3 was added and the flask temperature was increased to 100 ˚C followed by refluxing for 4 h. Then NH_2OH (3.0 mmol) and toluene (solvent) were added to the reaction mixture and the mixture was further refluxed for 30 min. At the end of the reaction, the solvent was evaporated and "2,4-dibromo-N-hydroxy-4-phenylbutanamide" was collected (Djerassi, 1948; Furniss et al., 1989; Niu et al., 2009).

2.1.4. Synthesis of final products (1-14): 2,4-Dibromo-N-hydroxybutanamide (1.1 mmol) and 2,4-dibromo-N-hydroxy-4-phenylbutanamide (1.1 mmol) were mixed with caffeoyl amide derivatives (1.0 mmol) separately and K_2CO_3 (1.1 mmol) was then added. This phase was carried out using the microwave, the temperature was adjusted to 120 ˚C, and power was kept at 90 watts for 20 min duration. Thereafter extraction of the organic fraction was done using ethyl acetate. In the end, the solvent was removed to collect the final product (Ju and Varma, 2006).

N-Hydroxy-1-[3-(3-hydroxyphenyl)prop-2-enoyl]azetidine-2-carboxamide (1): FTIR ν cm^{-1} (KBr): 3385.07 (O-H str., phenolic OH), 1670.35 (C=O str., CONH), 1259.52 (C-N str.), 3292.49 (N-H str.), 1597.06 (C=C

str., aromatic), 1670.35 (C=C str.), 2852.72 (C-H str.); ^{1}HNMR (δ ppm, DMSO): 2.4 (s, H of CH_2), 3.46 (s, H of CH_2), 3.70 (s, H of CH_2), 5.32 (s, H of phenolic OH), 6.72 (s, H of CH of phenyl), 7.16 (s, H of CH of phenyl), 7.54 (s, H of CH of phenyl), 7.320 (s, H of α-C to amide C=O), 7.62 (s, H of N-H of CONH), 2.524 (H of OH of NHOH).

N-Hydroxy-1-[3-(4-hydroxyphenyl)prop-2-enoyl]azetidine-2-carboxamide (2): FTIR ν cm^{-1} (KBr): 3201.83 (O-H str., phenolic OH), 1849.73 (C=O str.), 1247.94 (C-N str.), 3383.14 (N-H str.), 1444.68 (C=C str., aromatic), 1598.99 (C=C str.), 2850.79 (C-H str.).

N-Hydroxy-1-[3-(3-methoxyphenyl)prop-2-enoyl]azetidine-2-carboxamide (3): FTIR ν cm^{-1} (KBr): 3383.14 (N-H str.), 1660.71 (C=O str., amide), 1232.51 (C-N str.), 1581.63 (C=C str., aromatic), 1153.43 (-OCH_3 str.), 1622.71 (C=C str.), 2962.66 (C-H str.).

N-Hydroxy-1-[3-(4-methoxyphenyl)prop-2-enoyl]azetidine-2-carboxamide (4): FTIR ν cm^{-1} (KBr): 3491.61 (N-H str.), 1253.73 (C-N str., amide), 1676.14 (C=O str., amide), 2841.15 (C-H str.), 1429.25 (C=C str., aromatic), 1593.2 (C=C str.), 1163.08 (-OCH_3 str.).

N-Hydroxy-1-[3-phenylprop-2-enoyl]azetidine-2-carboxamide (5): FTIR ν cm^{-1} (KBr): 1417.68 (C=C str., aromatic), 3493.09 (N-H str.), 1629.85 (C=O str., amide), 1224.8 (C-N str., amide), 2837.29 (C-H str., aromatic), 1676.14 (C=C str., aromatic).

1-[3-(3,4-dimethoxyphenyl)prop-2-enoyl]-N-hydroxyazetidine-2-carboxamide (6): FTIR ν cm^{-1} (KBr): 1683.86 (C=O str., amide), 1259.52 (C-N str.), 3028.24 (N-H str.), 1458.18 (C=C str.), 2839.22 (C-H str.), 1139.93 (-OCH_3 str.), 1591.27 (C=C str., aromatic).

1-[3-(3-ethoxy-4-hydroxyphenyl)prop-2-enoyl]-N-hydroxyazetidine-2-carboxamide (7): FTIR ν cm^{-1} (KBr): 1259.52 (C-N str.), 1676.14 (C=O str., amide), 3491.16 (N-H str.), 3645.46 (O-H str., phenolic), 1591.27 (C=C str., aromatic), 1143.79 (-C_2H_5 str.), 1660.71 (C=C str.), 2839.22 (C-H str.); ^{1}HNMR (δ ppm, DMSO): 2.52 (s, H of CH_2), 3.42 (s, H of CH_2), 3.88 (s, H of CH_2), 5.52 (s, H of phenolic OH), 6.40 (s, H of CH), 7.64 (s, H of CH), 7.16 (s, H of CH), 7.42 (s, H of α-C to amide carbonyl), 7.78 (s, H of N-H of CONH), 2.524 (H of O-H of NHOH), 4.10 (s, H of methylene), 1.34 (s, H of methyl).

N-Hydroxy-1-[3-(3-hydroxyphenyl)prop-2-enoyl]-3-phenylazitidine-2-carboxamide (8): FTIR ν cm^{-1} (KBr): 3390.86 (O-H str., phenolic), 1273.02 (C-N str.), 3390.86 (N-H str.), 1637.56 (C=O str., amide), 2926.01 (C-H str., aromatic), 1452.4 (C=O str., aromatic).

N-Hydroxy-1-[3-(4-hydroxyphenyl)prop-2-enoyl]-3-phenylazitidine-2-carboxamide (9): FTIR ν cm^{-1} (KBr): 3412.08 (O-H str., phenolic), 1581.63 (C=O str., amide), 1450.47 (C=C str., aromatic), 2926.01 (C-H str., aromatic), 1249.87 (C-N str.); ^{1}HNMR (δ ppm, DMSO): 2.60 (s, H of CH_2 of azetidine), 3.40 (s, H of CH_2 of azetidine), 5.46 (s, H of CH_2 of azetidine), 5.52 (s, H of phenolic OH), 6.32 (d, 2H of CH), 7.12 (d, 2H of CH), 7.52 (s, H of α-C to amide carbonyl), 7.92 (s, H of NH of CONH), 2.54 (H of OH of hydroxamate), 7.32 (d, 2H of phenyl), 7.42 (t, 3H of phenyl).

N-Hydroxy-1-[3-(3-methoxyphenyl)prop-2-enoyl]-3-phenylazitidine-2-carboxamide (10): FTIR ν cm^{-1} (KBr): 1676.14 (C=O str., amide), 1230.58 (C-N str.), 3394.72 (N-H str.), 1159.22 (-OCH_3 str.), 1581.63 (C=C str., aromatic), 3055.24 (C-H str., aromatic), 1629.85 (C=C str.).

N-hydroxy-1-[3-(4-methoxyphenyl)prop-2-enoyl]-3-phenylazitidine-2-carboxamide (11): FTIR ν cm^{-1} (KBr): 1676.14 (C=O str., amide), 3396.64 (N-H str., amide), 1595.13 (C=C str., aromatic), 3020.53 (C-H str., aromatic), 1629.85 (C=C str., aromatic).

N-Hydroxy-1-[3-phenylprop-2-enoyl]-3-phenylazitidine-2-carboxamide (12): FTIR ν cm^{-1} (KBr): 1581.63 (C=C str., aromatic), 3024.38 (C-H str., aromatic), 3061.24 (N-H str.), 1280.73 (C-N str., amide), 1676.14 (C=O str., amide), 1629.85 (C=C str., aromatic).

1-[3-(3,4-Dimethoxyphenyl)prop-2-enoyl]-N-hydroxy-3-phenylazitidine-2-carboxamide (13): FTIR ν cm^{-1} (KBr): 1257.59 (C-N str.), 3323.35 (N-H str., amide), 1676.14 (C=O str., amide), 1456.26 (C=C str., aromatic), 1138 (OCH_3 str.) 3026.31 (C-H str., aromatic), 1629.85 (C=C str.).

1-[3-(3-ethoxy-4-hydroxyphenyl)prop-2-enoyl]-N-hydroxy-3-phenylazitidine-2-carboxamide (14): FTIR ν cm^{-1} (KBr): 3402.43 (OH str., phenolic OH), 1139.93 (-OC_2H_5 str.), 1678.07 (C=O str., amide), 1259.52 (C-N str.), 2927.94 (N-H str.), 1591.27 (C=C str., aromatic), 1652.99 (C=C str.); ^{1}HNMR (δ ppm, DMSO): 3.42 (s, H of CH_2 of azetidine), 3.54 (s, H of CH_2 of azetidine), 3.82 (s, H of CH_2 of azetidine), 6.40 (s, H of CH), 6.46 (s, H of CH), 7.90 (s, H of NH of CONH), 2.54 (H of O-H of NHOH), 7.30 (d, 2H of phenyl), 7.44 (t, 3H of phenyl), 3.80 (d, 2H of OCH_3).

2.2. Docking studies

In silico molecular docking was performed for the designed compounds in the binding site of the NDM-1 enzyme (PDB ID: 4U4L) using AutoDock Vina and AutoDock Tools (ADTs) (Trott and Olson, 2010; Morris et al., 2009). The methodology employed to carry out the docking of designed analogues with the NDM-1 enzyme is depicted in Figure 1 (Miteva et al., 2010; Grewal et al., 2018; Rathee et al., 2018; Grewal et al., 2019; Rathee et al., 2019; Chauhan et al., 2020).

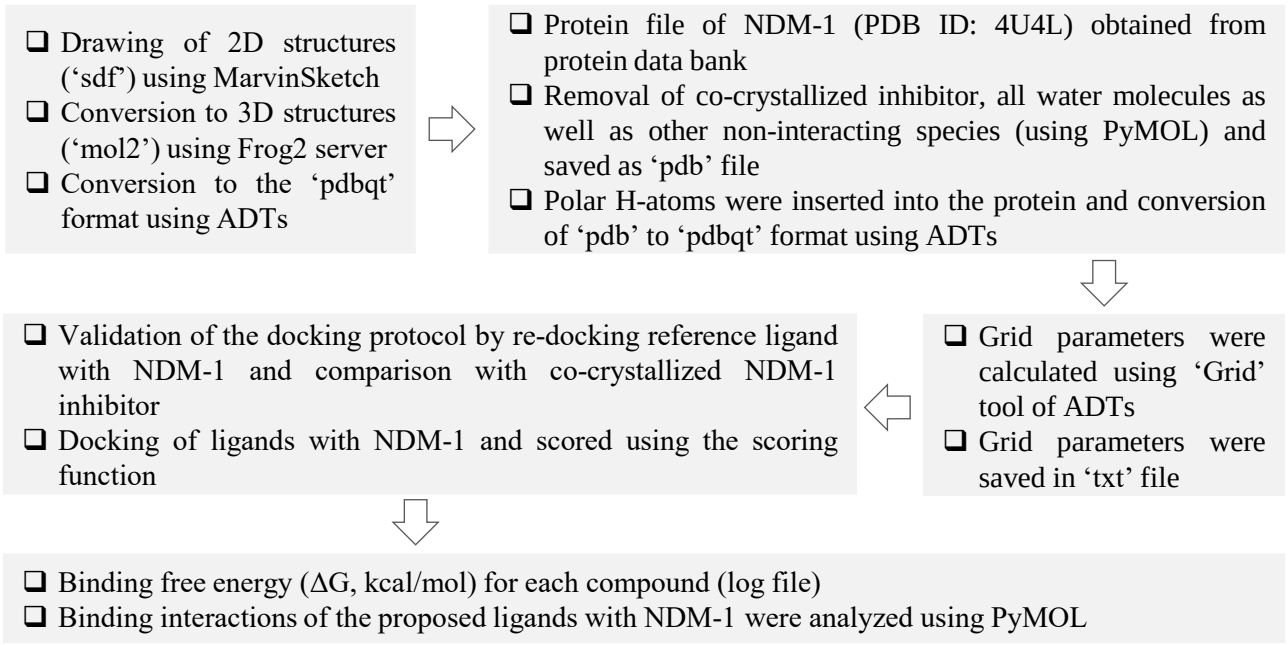

Figure 1. The methodology employed for the molecular docking of the designed analogues with NDM-1.

2.3. Evaluation of antibacterial potential

The procedure used for the evaluation of the antibacterial potential of the synthesized compounds is presented in Figure 2 (Upadhyay et al., 2010; Sharifi-Rad et al., 2015).

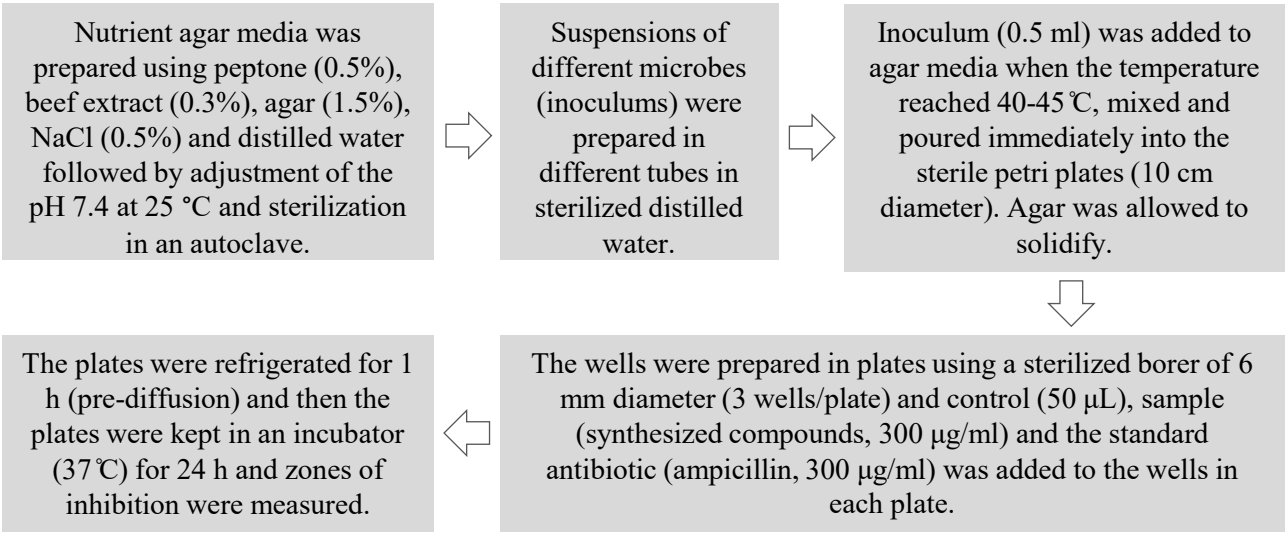

Figure 2. The procedure used for the evaluation of the antibacterial potential of the synthesized compounds.

3. Results and Discussion

3.1. Chemistry

The synthesis of the azetidine-substituted caffeic acid analogues was performed as depicted in Scheme 1. The purity of the synthesized derivatives was checked through "single spot TLC on silica gel G plates" and was further established via their steady FTIR and ^{1}H-NMR spectra that endorsed the synthesis as well as purity constraints of the synthesized molecules. The physicochemical properties of the synthesized molecules are given in Table 1.

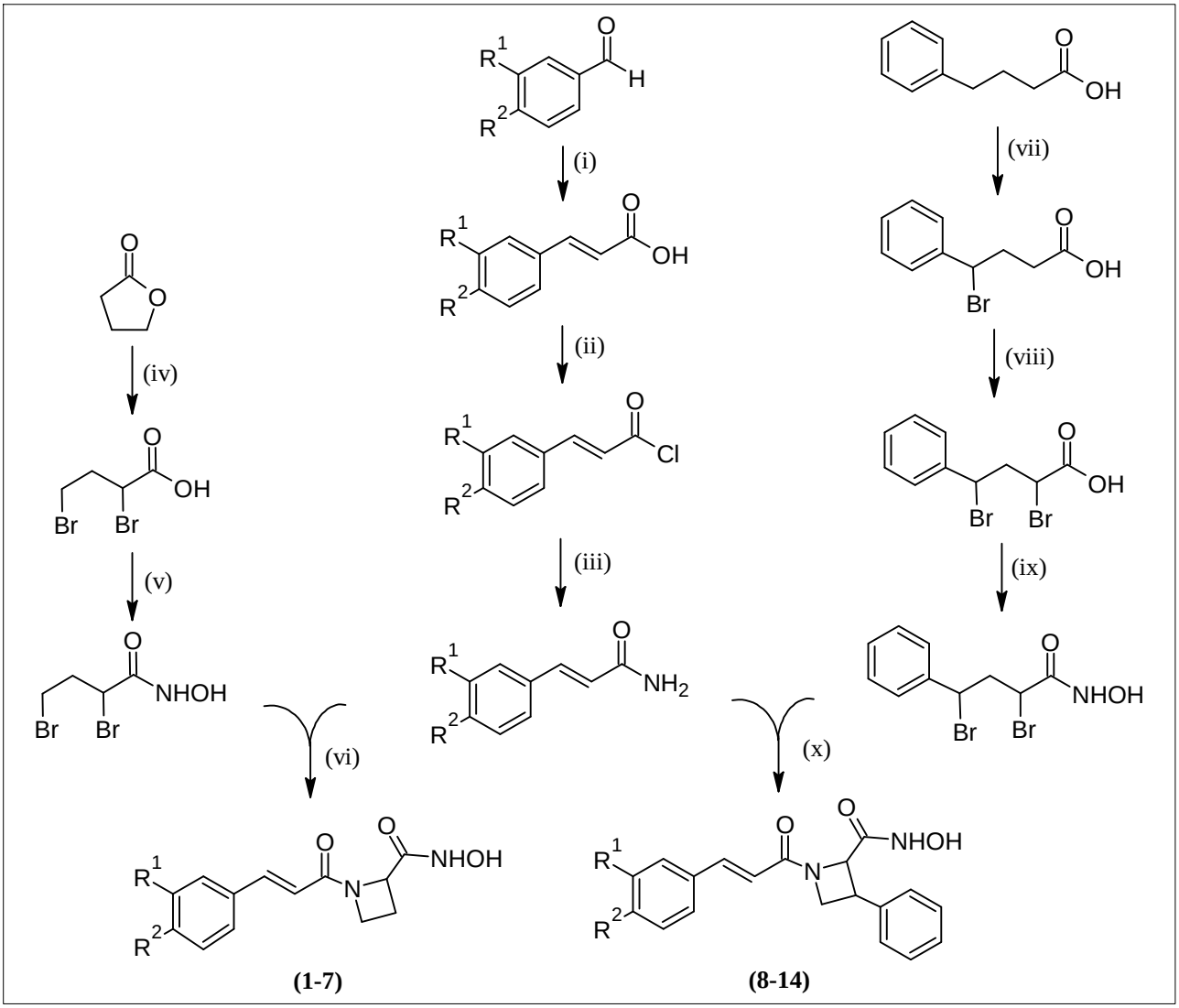

Scheme 1. Procedure for synthesis of azetidine substituted caffeic acid analogues. **Reagents and conditions**: (i) $CH_2(COOH)_2$, C_6H_5N, 55 ˚C, 3 h; (ii) $SOCl_2$, 4 h; (iii) Ammonia, 3 h; (iv) Bromine, PBr_3, reflux, 4 h; (v) NH_2OH, reflux, 30 min; (vi) K_2CO_3, 120 ºC, 90 W, Microwave, 20 min; (vii) 1-Bromo-2,5-pyrrolidinedione, $(C_6H_5C(=O)O)_2$, 25 min; (viii) Bromine, PCl_3, reflux, 4 h; (ix) NH_2OH, reflux, 30 min; (x) K_2CO_3, 120 ºC, 90 W, Microwave irradiation, 20 min.

Table 1. Physicochemical parameters of the synthesized azetidine substituted caffeic acid analogues.

Compound	R^1	R^2	Mol. Formula	Mol. Weight	Melting Point (˚C)	R_f*	% Yield
1	-OH	-H	$C_{13}H_{14}N_2O_4$	262.26	128-130	0.59	64
2	-H	-OH	$C_{13}H_{14}N_2O_4$	262.26	98-100	0.60	61
3	$-OCH_3$	-H	$C_{14}H_{16}N_2O_4$	276.29	152-154	0.62	55
4	-H	$-OCH_3$	$C_{14}H_{16}N_2O_4$	276.29	140-142	0.64	58
5	-H	-H	$C_{13}H_{14}N_2O_3$	246.26	127-129	0.78	54
6	$-OCH_3$	$-OCH_3$	$C_{15}H_{18}N_2O_5$	306.31	144-146	0.54	52
7	$-OC_2H_5$	-OH	$C_{15}H_{18}N_2O_5$	306.31	138-140	0.49	54

8	-OH	-H	$C_{19}H_{18}N_2O_4$	338.36	128-130	0.67	50
9	-H	-OH	$C_{19}H_{18}N_2O_4$	338.36	124-126	0.51	44
10	$-OCH_3$	-H	$C_{20}H_{20}N_2O_4$	352.39	137-139	0.58	61
11	-H	$-OCH_3$	$C_{20}H_{20}N_2O_4$	352.39	141-143	0.69	51
12	-H	-H	$C_{19}H_{18}N_2O_3$	322.36	153-155	0.80	58
13	$-OCH_3$	$-OCH_3$	$C_{21}H_{22}N_2O_5$	382.41	133-135	0.76	45
14	$-OC_2H_5$	-OH	$C_{21}H_{22}N_2O_5$	382.41	153-155	0.68	51

The ^{1}H-NMR spectra of the synthesized analogues showed the "NH" peak at about δ 8.0 ppm verifying the hydroxamate (-NHOH) moiety. The ^{1}H-peak of the heterocyclic ring was observed at about δ 2.0 ppm, verifying the presence of a four-membered heterocyclic ring. The ^{1}H-NMR spectra of the synthesized compounds showed singlet around δ 6.50 ppm confirming the presence of H on α-C to amide carbonyl and singlet around δ 7.50 ppm H on β-C to amide carbonyl. The methoxy groups were verified by the peak at about δ 4.0 ppm as seen in the ^{1}H-NMR spectrum of compound 6. The protons associated with the aromatic scaffold were detected with the expected chemical shift and integral values. The FTIR spectra of the analogues unveiled absorption bands in the range of 1335 cm^{-1} to 1220 cm^{-1} equivalent to aromatic nitrogen hence verifying the occurrence of a heterocyclic scaffold. Absorption bands in the range 1600-1475 cm^{-1} corresponding to the C=C stretching band indicate the presence of aromatic rings in the synthesized compounds. The C-C stretching in region 1680-1600 cm^{-1} showed the occurrence of an aliphatic chain. Stretching in the range 1175-1060 cm^{-1} matched to C-O of the methoxy and ethoxy groups. The absorption band in the region 3500-3100 cm^{-1} revealed the presence of N-H stretch. The absorption bands in the region 1680-1630 cm^{-1} confirmed the presence of C=O in the amide group. The presence of the phenolic -OH group was verified by the absorption band in the range 3600-3550 cm^{-1} of the phenyl ring.

3.2. Docking studies

Lead optimization of the designed analogues was carried out through the prediction of drug-likeness properties (molecular weight (Mol. Weight), partition coefficient (log P), hydrogen bond donors (HBA), and hydrogen bond acceptors (HBD)). Most of the molecules chosen for *in silico* investigation possessed "drug-like properties" as derived from "Lipinski's rule of five" (Table 2). The docking simulations were performed using AutoDock Vina for the designed caffeic acid derivatives in the binding site of NDM-1 protein (PDB entry: 4U4L) and validated by re-docking of the 4U4L ligand in the active site (binding free energy, i.e., ΔG value of -7.2). The designed NDM-1 inhibitors were docked in the active site of NDM-1 protein comprising of catalytic zinc ions. Almost all the caffeic acid derivatives showed appreciable binding in the active site as determined by analysing the H-bond, metal interactions, hydrophobic interactions and binding free energy (ΔG) of the "best-docked poses". The docking simulations of the designed ligands proposed a complementary fit in the active site of the NDM-1 protein. The best-docked poses for all the caffeic acid derivatives were further analysed in detail using PyMOL.

Table 2. Molecular properties and docking score of best-docked poses of the synthesized azetidine substituted caffeic acid derivatives.

Compound	Mol. Weight	Log P*	HBA*	HBD*	ΔG (kcal/mol)
1	262.26	0.28	4	2	-6.9
2	262.26	0.28	4	2	-6.8
3	276.29	0.31	4	2	-7.0
4	276.29	0.31	4	2	-7.0
5	246.26	0.57	3	2	-7.1
6	306.31	0.06	5	2	-6.8
7	306.31	0.03	5	3	-6.9
8	338.36	2.00	4	2	-7.3
9	338.36	2.00	4	2	-7.7
10	352.39	2.03	4	2	-7.8
11	352.39	2.03	4	2	-7.4
12	322.36	2.29	3	2	-7.5
13	382.41	1.84	5	2	-7.6
14	382.41	2.05	5	3	-7.8

*Mol. Weight, HBA, HBD, and log P were calculated using Marvin Sketch (ChemAxon, Budapest).

The docked pose of compound 1 showed a weak hydrogen bond interaction of the carbonyl (C=O) group with NH_2 of Asn220 in the active site of NDM-1. The NH and OH of the 'NHOH' group also showed metal interactions with the Zn^{2+} ion of NDM-1. An overlap of the docked pose of compound 1 with that produced by the "4U4L ligand" exposed that compound 1 had a comparable binding pattern in the active site of the protein as that of the co-crystallized inhibitor (Figure 3). In a way to improve hydrogen bond interactions, metal interactions and hydrophobic interactions further structural modifications in compound 1 were carried out. The docked pose of compound 2 exposed a hydrogen bond interaction of the carbonyl group with NH_2 of Asn220 residue in the active site of the NDM-1 enzyme. The NH and OH of NHOH also showed metal interaction with the Zn^{2+} ion of NDM-1 (Figure 4).

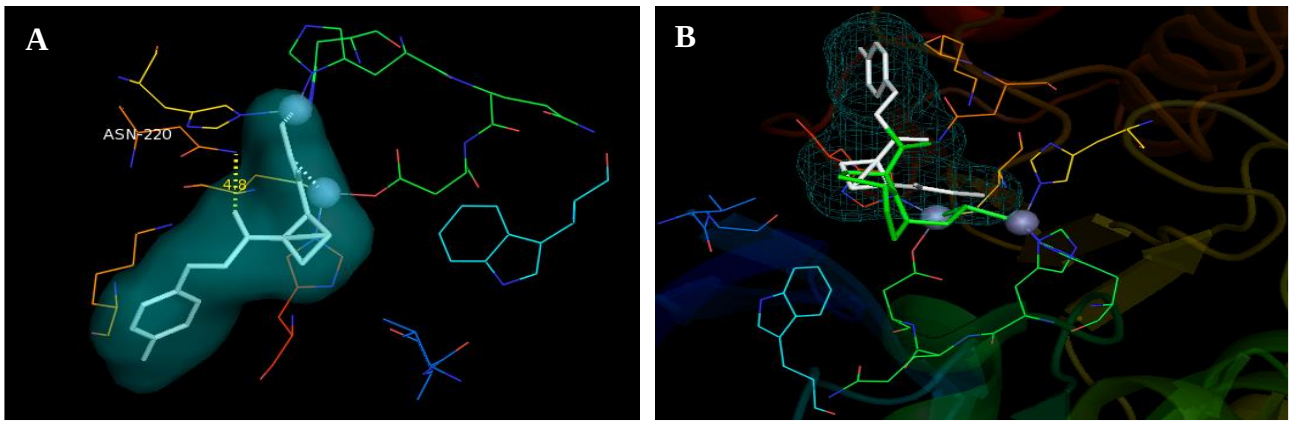

Figure 3. (a) Docked pose showing hydrogen bond interactions for compound 1 in the active site of NDM-1; (b) Overlay of the docked pose of compound 1 (white) with that produced by co-crystallized PDB Ligand 4U4L (green).

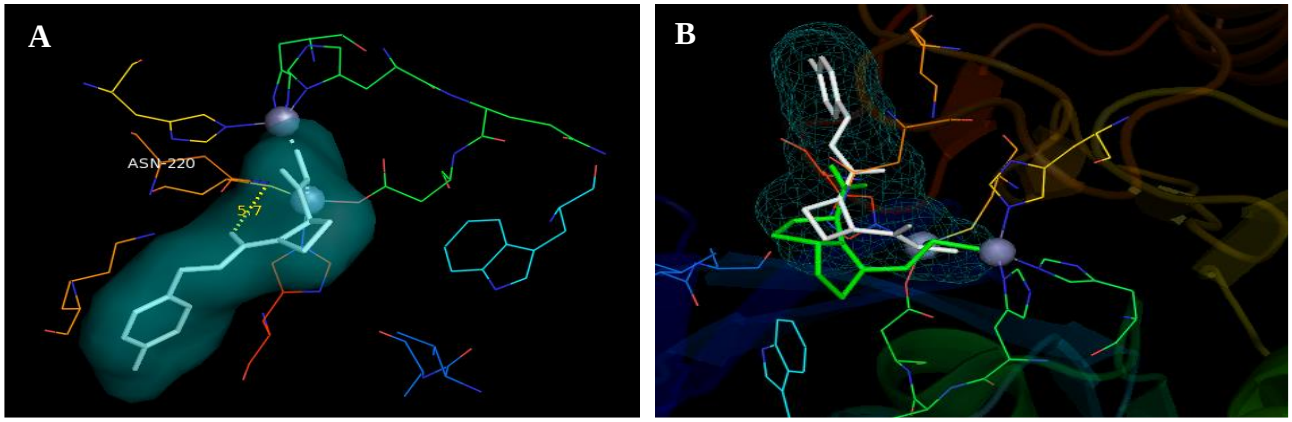

Figure 4. (a) Docked pose showing hydrogen bond interactions for compound 2 in the active site of NDM-1; (b) Overlay of the docked pose of compound 2 (white) with that produced by co-crystallized PDB Ligand 4U4L (green).

All the other designed molecules of the series (compounds 3-14) also exhibited similar binding patterns and orientation in the active site of the enzyme as that of the co-crystallized inhibitor as revealed from the docking poses and overlay of these compounds with reference ligand.

3.3. Antimicrobial activity

All the prepared molecules were screened for antibacterial action against *Escherichia coli* and *Pseudomonas aruginosa* strains in presence of ampicillin (Table 3).

Table 3. Preliminary antibacterial screening result of the synthesized compounds.

Compound	**Zone of Inhibition***	
	E. coli	***P. aeruginosa***
1	+++	+
2	++	+
3	++	++

4	++	+++
5	+	+
6	+++	++
7	++	++
8	++	+
9	+++	++
10	++	+
11	++	+
12	+	++
13	+	+++
14	+++	++
Control	+	+
Ampicillin	++	++

*Zone of inhibition (mm): + = 6-12 mm, ++ = 12-18 mm, +++ > 18 mm.

Compounds 1, 6, 9 and 14 showed better activities than the standard drug (ampicillin) wherever 2, 4, 7, 8, 10 and 11 produced equal activity as compared to the standard drug (ampicillin) against *E. coli*. Compounds 5, 12 and 13 showed weak antibacterial activity against *E. coli*. Compounds 4 and 13 showed better activity than the standard drug (ampicillin), whereas 3, 6, 7, 9, 12 and 12 produced equal activity as compared to the standard drug (ampicillin) against *P. aeruginosa*. Compounds 1, 2, 5, 8, 10 and 11 showed weak antibacterial activity against *P. aeruginosa*.

4. Conclusions

The present research work was planned to design and synthesize some novel potential NDM-1 inhibitors based on the caffeic acid nucleus. The structure-based drug design was used to design the molecules by utilizing the X-ray crystallographic information of NDM-1 from the PDB database. Based on the pharmacophoric requirements for the NDM-1 active site, the caffeic acid nucleus was selected for the design of some newer analogues and the hydroxamate group was introduced (to interact with Zn^{2+} through metal interaction) in the designed caffeic acid derivatives. The synthesized caffeic derivatives were evaluated *in silico* to evaluate their binding with the NDM-1 protein. These molecules were found to show an almost analogous binding pattern as that of the ligand selected from PDB with entry number 4U4L. The preliminary *in silico* and *in vitro* antimicrobial activity results show a huge potential of these caffeic acid derivatives to act as strong NDM-1 inhibitors for combating antibiotic resistance.

Acknowledgements

The authors are thankful to the Management, JCD Vidyapeeth, Sirsa, Haryana (India) for their support and encouragement for this research work.

Conflicts of Interest

The authors declare no conflict of interest.

References

Ambler RP, Daniel M, Fleming J, Hermoso JM, Pang C, Waley SG. (1985). The amino acid sequence of the zinc-requiring beta-lactamase II from the bacterium Bacillus cereus 569. FEBS Lett, 189(2), 207-211.

Aoki N, Ishii Y, Tateda K, Saga T, Kimura S, Kikuchi Y, Kobayashi T, Tanabe Y, Tsukada H, Gejyo F, Yamaguchi K. (2010). Efficacy of calcium–EDTA as an inhibitor for metallo-β-lactamase in a mouse model of Pseudomonas aeruginosa pneumonia. Antimicrob Agents Chemother, 54, 4582-4588.

Chauhan A, Grewal AS, Pandita D, Lather V. (2020). Novel cinnamic acid derivatives as potential PPARδ agonists for metabolic syndrome: design, synthesis, evaluation and docking studies. Curr Drug Discov Technol, 17(3), 338-347.

Djerassi, C. (1948). Brominations with N-bromosuccinimide and related compounds; the Wohl-Ziegler Reaction. Chem Rev, 43(2), 271-317.

Fair RJ, Tor Y. (2014). Antibiotics and bacterial resistance in the 21st century. Perspect Medicin Chem, 6, 25-64.

Furniss BS, Hannaford AJ, Smith PWG, Tatchell AR. (1989). Vogel's Textbook of Practical Organic Chemistry. Pearson Education, New Delhi.

Grewal AS, Kharb R, Prasad DN, Dua JS, Lather V. (2019). Design, synthesis and evaluation of novel 3,5-disubstituted benzamide derivatives as allosteric glucokinase activators. BMC Chem, 13(1), 2.

Grewal AS, Lather V, Pandita D, Bhayana G. (2017). Synthesis, docking and evaluation of phenylacetic acid and trifluoro-methylphenyl substituted benzamide derivatives as potential PPARδ Agonists. Lett Drug Des Discov, 14(11), 1239-1251.

Grewal AS, Sharma K, Singh S, Singh V, Pandita D, Lather V. (2018). Design, Synthesis and Antidiabetic Activity of Novel Sulfamoyl Benzamide Derivatives as Glucokinase Activators. J Pharm Technol Res Manag, 6(2), 113-122.

Grewal AS, Thapa K, Sharma N, Singh S. (2020). New Delhi metallo-β-lactamase-1 inhibitors for combating antibiotic drug resistance: recent developments. Med Chem Res, 29(1), 1301-1320.

Hawkey PM. (2015). Multidrug-Resistant gram-negative bacteria: a product of globalization. J Hosp Infect, 89, 241-247.

Johnson AP, Woodford N. (2013). Global spread of antibiotic resistance: the example of New Delhi metallo-β-lactamase (NDM)-mediated carbapenem resistance. J Med Microbiol, 62(Pt 4), 499-513.

Ju Y, Varma RS. (2006). Aqueous N-heterocyclization of primary amines and hydrazines with dihalides: microwave-assisted syntheses of N-Azacycloalkanes, isoindole, pyrazole, pyrazolidine, and phthalazine derivatives. J Org Chem, 71(1), 135-141.

Kavitha, J., Rajashekher, D., Subbaraju, V. G., & Ramesh, G. N. (1999). Synthesis of vinyl caffeate, an antioxidant from Perilla frutescens Britton var. crispa (Thunb.). Indian J Chem B, 38B(11), 1280-1281.

King DT, Strynadka NC. (2013). Targeting metallo-β-lactamase enzymes in antibiotic resistance. Future Med Chem, 5, 1243-1263.

Kumar A, Grewal AS, Singh V, Narang R, Pandita D, Lather V. (2018). Synthesis, antimicrobial activity and QSAR studies of some new sparfloxacin derivatives. Pharm Chem J, 52(5), 444-454.

Kumarasamy KK, Toleman MA, Walsh TR, Bagaria J, Butt F, Balakrishnan R, Chaudhary U, Doumith M, Giske CG, Irfan S, Krishnan P, Kumar AV, Maharjan S, Mushtaq S, Noorie T, Paterson DL, Pearson A, Perry C, Pike R, Rao B, Ray U, Sarma JB, Sharma M, Sheridan E, Thirunarayan MA, Turton J, Upadhyay S, Warner M, Welfare W, Livermore DM, Woodford N. (2010). Emergence of a new antibiotic resistance mechanism in India, Pakistan, and the UK: a molecular, biological, and epidemiological study. Lancet Infect Dis, 10(9), 597-602.

Linciano P, Cendron L, Gianquinto E, Spyrakis F, Tondi D. (2019). Ten years with New Delhi metallo-β-lactamase-1 (NDM-1): from structural insights to inhibitor design. ACS Infect Dis, 5(1), 9-34.

Liu Z, Wang Y, Walsh TR, Liu D, Shen Z, Zhang R, Yin W, Yao H, Li J, Shen J. (2017). Plasmid-mediated novel blaNDM-17 gene encoding a carbapenemase with enhanced activity in a sequence type 48 Escherichia coli strain. Antimicrob Agents Chemother, 61(5), e02233-16.

Miteva MA, Guyaon F, Tuffery P. (2010). Frog2: Efficient 3D conformation ansemble generator for small compounds. Nucleic Acids Res, 38, W622-W627.

Morris GM, Huey R, Lindstrom W, Sanner MF, Belew RK, Goodsell DS, Olson AJ. (2009). AutoDock4 and AutoDockTools4: automated docking with selective receptor flexibility. J Comput Chem, 30(16), 2785-2791.

Niu T, Zhang W, Huang D, Xu C, Wang H, Hu Y. (2009). A powerful reagent for synthesis of Weinreb amides directly from carboxylic acids. Org Lett, 11(19), 4474-4477.

Papst L, Beović B, Pulcini C, Durante-Mangoni E, Rodríguez-Baño J, Kaye KS, Daikos GL, Raka L, Paul M, ESGAP, ESGBIS, ESGIE & the CRGNB Treatment Survey Study Group. (2018). Antibiotic treatment of infections caused by carbapenem-resistant Gram-negative bacilli: an international ESCMID cross-sectional survey among infectious diseases specialists practicing in large hospitals. Clin Microbiol Infect, 24(10), 1070-1076.

Rathee D, Lather V, Grewal AS, Dureja H. (2018). Targeting matrix metalloproteinases with novel diazepine substituted cinnamic acid derivatives: design, synthesis, in vitro and in silico studies. Chem Cent J, 12(1), 41.

Rathee D, Lather V, Grewal AS, Dureja H. (2019). Enzymatic inhibitory activity of iridoid glycosides from Picrorrhiza kurroa against matrix metalloproteinases: correlating in vitro targeted screening and docking. Comput Biol Chem, 2019, 78, 28–36.

Rogers BA, Sidjabat HE, Silvey A, Anderson TL, Perera S, Li J, Paterson DL. (2013). Treatment options for New Delhi metallo-beta-lactamase-harboring enterobacteriaceae. Microb Drug Resist, 19(2), 100-103.

Rotondo CM, Wright, G. D. (2017). Inhibitors of Metallo-β-Lactamases. Current Opinion in Microbiology, 39, 96–105.

Sharifi-Rad J, Hoseini-Alfatemi SM, Sharifi-Rad M, Sharifi-Rad M, Iriti M, Sharifi-Rad M, Sharifi-Rad R, Raeisi S. (2015). Phytochemical compositions and biological activities of essential oil from Xanthium strumarium L. Molecules, 20(4), 7034-7047.

Shi C, Chen J, Xiao B, Kang X, Lao X, Zheng H. (2019). Discovery of NDM-1 inhibitors from natural products. J Glob Antimicrob Resist, 18, 80-87.

Shlaes DM. (2013). New β-Lactam–β-lactamase inhibitor combinations in clinical development. Ann N Y Acad Sci, 1277, 105-114.

Sidjabat H, Nimmo GR, Walsh TR, Binotto E, Htin A, Hayashi Y, Li J, Nation RL, George N, Paterson DL. (2011). Carbapenem resistance in Klebsiella pneumoniae due to the New Delhi Metallo-β-lactamase. Clin Infect Dis, 52(4), 481-484.

Tang SS, Apisarnthanarak A, Hsu LY. (2014). Mechanisms of β-lactam antimicrobial resistance and epidemiology of major community- and healthcare-associated multidrug-resistant bacteria. Adv Drug Deliv Rev, 78, 3-13.

Trott O, Olson AJ. (2010). AutoDock vina: improving the speed and accuracy of docking with a new scoring function, efficient optimization and multithreading. J Comput Chem, 31(2), 455-461.

Upadhyay RK, Dwivedi P, Ahemad S. (2010). Screening of antibacterial activity of six plant essential oils against pathogenic bacterial strains. Asian J Med Sci, 2(3), 152-158.

Wagner AF, Walton E, Hoffman CH, Peterson LH, Holly FW, Folkers K. (1955). Synthesis of DL-Dimethyldihydro-α-Lipoic Acid. J Am Chem Soc, 77(19), 5140-5143.

How to cite this article: Verma M, Grewal AS, Pandita D, Lather V. Design and synthesis of a newer series of caffeic acid derivatives as potential New Delhi metallo-β-lactamase-1 (NDM-1) inhibitors. Pharma Research Bulletin, 2021, 3(1), 08-17.